Understanding the driving factors (precipitation variation, land use changes and check dams) and mechanisms behind the changes in sediment load of a Loess watershed, China

Xiang Zhang[1], Dongli She[2], and Guangbo Wang[2]

[1] State Key Laboratory of Soil Erosion and Dryland Farming on the Loess Plateau
[2]Key Laboratory of Efficient Irrigation-Drainage and Agricultural Soil-Water Environment in Southern China, Ministry of Education

September 28, 2020

Abstract

Soil and water conservation measures, especially reforestation and check dam construction, have been progressively implemented on the coarse sandy hilly catchment region of the Yellow River basin for several decades, and climate conditions are also dynamic. Therefore, it is very urgent to understand how the precipitation variation, land use changes and check dams affect soil erosion and sediment yield in a large watershed. The sediment delivery distributed (SEDD) model was employed to quantitatively identify the impacts of the three factors on soil erosion and sediment yield in the Kuye River watershed. Significant land use changes, with the conversion of arable land and bare land to vegetation cover and construction land, occurred in the study watershed from 1987 to 2016. In addition, 306 key dams were built in the watershed, with a total storage capacity of 316.64 Mm3, according to the statistical data of 2011. Hot spot analysis showed that the high-risk regions for soil erosion and sediment yield were mainly concentrated in the middle reaches of the watershed. The simulation results showed that the check dams were the dominant factor, reducing total sediment load by 53.77% in 2006. However, from 1987 to 2016, the contribution of these three factors (precipitation variation, land use changes and check dams) to sediment reduction was 29.10%, 40.09% and 30.81%, respectively, which indicated that all of them had significant influence on sediment load. The results can serve as a reference for watershed management and policy implementation.

1. INTRODUCTION

Soil erosion is wide-ranging worldwide and has irreversible effects on all-natural and artificial ecosystems (Fu et al., 2011). It is not only the primary cause of soil deterioration (Marques et al., 2008), land productivity decline (Lantican et al., 2003), and degradation of rivers, lakes and estuaries but also often carries sediments and pollutants. Soil erosion has accelerated approximately 85% of global land degradation and resulted in a 17% reduction in food production (Tang et al., 2015), which has become one of the most serious societal and environmental problems in the world.

The middle and upper reaches of the Yellow River basin are located on the Loess Plateau of China. Owing to its unique soil characteristics, climate conditions and extremely fragile ecosystem (Wang et al., 2017; Xin et al., 2012), the Loess Plateau is a global hot spots of soil erosion. Approximately 40% of the whole Loess Plateau suffers from extremely high erosion, and the annual soil erosion modulus is more than 5000 t/km^2 (Fu et al., 2011), which increases the risk of soil degradation and restricts the sustainable development of the ecosystem (Zhao et al., 2016). The high-risk areas are mainly concentrated in hilly and gully loess areas (Chen et al., 2007), which are the main source of Yellow River sediment. Since the 1950s, to control severe soil erosion, the government has issued many policies and implemented a series of soil conservation measures

for the Loess Plateau. The control of soil and water loss on the Loess Plateau can be divided into two parts, namely, slope vegetation restoration (i.e., reforestation) and gully control (i.e., check dams).

As a main measure for reducing erosion, vegetation restoration has been widely used on the Loess Plateau, especially since the implementation of the 'Grain for Green' project. The increase in vegetation coverage can effectively control soil erosion through root consolidation of soil, increased infiltration, and reduced surface runoff and water flow velocity (Bruijnzeel, 2004), improving the resistance of the soil erosion and reducing water erosion capacity and sediment transport capacity (Rey et al., 2005; Vanacker et al., 2007). At the same time, the variation in vegetation cover will directly lead to changes in land use. In fact, land use changes will be affected by human activities, such as the implementation of policies and urban development and its impact on soil erosion is bidirectional. Changes in land use may not only lead to sediment reduction (Choukri et al., 2020) but also increase soil erosion and further lead to land degradation (Aneseyee et al., 2020). For example, Quiñonero-Rubio et al. (2016) used the WaTEM/SEDEM model to simulate the Upper Taibilla catchment of Spain and indicated that afforestation reduced sediment yield by 13.9% (1956-2000). Aneseyee et al. (2020) demonstrated that land use changes increased soil loss by 26.25% and sediment export by 3.45% (1988-2018), mainly due to the expansion of urbanization and reclamation.

The construction of check dams has become an effective soil and water conservation measure for sediment control. A large number of check dams have been constructed in the gully channel to intercept the sediment, block floods, and reduce downstream scouring (Ran et al., 2008). When the check dams are fully filled, the main component of the land behind check dams is surface soil that is rich in nutrients, and its fertility is much higher than that of sloped farmland. According to reports, approximately 3200 $km^2$of dam croplands were formed in 2002 (Jin et al., 2012). Moreover, check dams effectively prevent sediment from entering the Yellow River, thus reducing the sediment concentration of the Yellow River (Ran et al., 2008). Although not widely used worldwide, check dams have been applied to control soil erosion and have been reported in France, the United States, Spain, China and elsewhere (Abedini et al., 2012; Bellin et al., 2011; Borja et al., 2018; Castillo et al., 2007; Fang, 2017). Polyakov et al. (2014) carried out field sampling in the Santa Rita Experimental Range in the United States and found that the check dams retained 50% of sediment yield. By measuring the sediment deposition within the gully channels of the Loreto catchment in the Andean Mountains, Borja et al. (2018) indicated that check dams reduced the sediment exported by more than 70%. Boix-Fayos et al. (2008) applied the WATEM-SEDEM model to the Rogativa catchment of Spain and showed that check dams reduced the sediment load by approximately 77% without land use changes. Xu et al. (2013) explored the interception benefit of check dams in the Yanhe River watershed and revealed that the proportional reduction in sediment reached from 34.6-48.0% in the rainy season (1984-1987) and increased to between 79.4 and 85.5% from 2006-2008.

In the past few decades, the Loess Plateau has also undergone varying degrees of climate change, in which precipitation variation plays a leading role in soil erosion. Sun et al. (2015) analyzed the precipitation changes of the Loess Plateau from 1961 to 2011, and found that the amount of precipitation in most areas showed a downward trend. In addition, over the past six decades, the sediment concentration of the Yellow River has decreased substantially (Wu et al., 2020), and the main tributaries in the middle reaches of the Yellow River have reported that sediment load has decreased rapidly (Gao et al., 2017; Rustomji et al., 2008; Yue et al., 2014). Hence, it is particularly important to understand the driving factors and mechanisms behind the changes in soil erosion and sediment load, which is also a prerequisite for sustainable watershed management (Montgomery, 2007).

To quantitatively identify the impact of the three factors (precipitation variation, land use changes and check dams), the Kuye River watershed, with an area of 8651 km^2 on the Loess Plateau, was selected as the study area by combining field investigations with model simulation. The main objectives of this study were to (1) explore the characteristics of soil erosion and sediment yield and to (2) quantify the contribution of precipitation variation, check dam construction and man-made land use changes to sediment reduction in the Kuye River watershed, which is a typical watershed in the coarse sandy hilly catchment region of the Yellow River basin.

2. MATERIALS AND METHODS

2.1 Description of study area

The Kuye River (*Fig. 1*) is a first-order tributary of the middle Yellow River, which flows through Inner Mongolia and Shaanxi and finally flows into the Yellow River. The area of the Kuye River watershed (38°22'–39deg50' N, 109deg28'–110deg45' E) is 8651 km^2, with a mainstream length of 242 km and an average channel slope of 2.6The elevation ranges from 713 m in the southeast to 1575 m in the northwest. There are two main tributaries (Wu-lan-mu-lun and Bei-niuchuan) in the upper reach of the watershed, and the Wenjiachuan hydrometrical station is located at the outlet of the Kuye River. The watershed has a typical arid to semiarid continental climate, with a multiyear average precipitation and temperature of 415 mm and 7.9degC, respectively. The average annual evaporation is 1788 mm. Intense storms mainly take place in July and August, accounting for more than 52% of the annual rainfall. Therefore, local short-term floods often occur in the watershed during this period. According to the measured data of the Wenjiachuan hydrological station, the sediment load in July and August accounts for 90% of the annual total (Cai et al., 2019).

Due to the sparse vegetation cover, loose soil, terrain fragmentation and dense gullies in this watershed, it has become one of the main sources of sediment in the Yellow River. The average annual sediment load measured at the Wenjiachuan hydrological station from 1954 to 2000 was 1.00x10^8 t (10800 t/km^2/a) (Rustomji et al., 2008). However, the observed sediment load decreased significantly over the past six decades. Compared with the 1960–1999 period, the average annual runoff and sediment discharge from 2000–2016 decreased by 76.72% and 94.50%, respectively (Zhao et al., 2019).

2.2 Datasets

The daily precipitation records of 50 rainfall stations and the daily sediment concentration data of the Wenjiachuan gauge in 1987 and from 2006-2016 were obtained from the "Hydrological Yearbook of the People's Republic of China - Hydrological Data of the Yellow River Basin".

The digital elevation map (DEM) came from the Geospatial Data Cloud, with a spatial resolution of 30 m (www.gscloud.cn). The DEM of the Kuye River watershed was extracted with the hydrological analysis tool in ArcGIS 10.2 (ESRI).

The land use scenarios for 1987 and 2006 were derived from the Landsat 5 Thematic Mapper (TM) remote sensing images downloaded from the United States Geological Survey (USGS) (https://glovis.usgs.gov/), while those for 2016 were from the Geospatial Data Cloud website (www.gscloud.cn). Then, a hybrid land use classification technique, which involved unsupervised classification and visual interpretation, was used. Unsupervised classifications were carried out using the iterative self-organizing data analysis (ISODATA) clustering algorithm, while visual interpretation was mainly employed using Google Earth's historical orthophoto images of corresponding years. To ensure the quality and accuracy of the data, field investigations and in-depth consultations with local elders were undertaken. Seven land use types were identified: forests, grassland, shrubland, bare land, arable land, water bodies and urban and mining areas.

2.3 Model description

The sediment delivery distributed (SEDD) model has been extensively used in different regions of the world. The model is mainly based on the RUSLE model and integrates GIS techniques to predict the sediment yield within a watershed. The SEDD (Ferro and Minacapilli, 1995) model estimates the sediment yield according to the following formula:

$$\mathrm{SY}_i = \mathrm{SE}_i \bullet \mathrm{SDR}_i = R_i \bullet K_i \bullet \mathrm{LS}_i \bullet C_i \bullet P_i \bullet \mathrm{SDR}_i \quad (1)$$

where SE_i is the average of annual soil erosion modulus (t/ha/a) on pixel i ; SDR_i is the sediment delivery ratio for pixel i ; $R_i$refers to the rainfall-runoff erosivity factor (MJ*mm/ha*h);K_i denotes the soil erodibility factor (t*ha*h/MJ*ha*mm); LS_i expresses the topographic factor; C_i signifies the cover-management factor; and P_i shows the support practice factor.

To explain the relationship between rainfall and erosion, Wischmeier and Smith (1978) proposed the R factor to quantify the impact of rainfall and runoff on soil erosion. Since the daily rainfall data of 50 rainfall stations were available, the method proposed by Zhang et al. (2002) was used to calculate the R factor, which was mainly assessed with the daily rainfall data using a half-month rainfall erosivity model. The annual R factor was generated by kriging interpolation using data from 50 rainfall stations, and the raster of the R factor in 2006 is shown in*Fig. 2* a.

The soil erodibility factor was applicable to characterize the sensitivity of soil to water erosion (Rao et al., 2014). Based on the soil map (1:500,000 scale) of the Loess Plateau and the revised erosion/productivity impact calculator (EPIC) model (Williams et al., 1984), the value of the soil erodibility factor was derived (*Fig. 2* b).

The LS factor is an index for measuring the impact of topography on soil erosion. As the Kuye River watershed was located on the Loess Plateau, which has complicated terrain, the terrain factor calculation tool 2.0 developed by Fu et al. (2015) for the Loess Plateau was imposed to calculate the LS factor (*Fig. 2* c). The DEM was adopted as the main data source for this calculation tool.

The cover-management factor reflects the effect of soil management on soil erosion rates, which are mainly related to land use type, vegetation cover, surface roughness and soil moisture (Renard et al., 1997). In this paper, the method proposed by Cai et al. (2000) was used to evaluate the C factor by integrating the normalized vegetation index (NDVI), which was obtained from remote sensing images of different periods of the Kuye River watershed (*Fig. 2* d).

The P factor represents the influence of supporting measures on sediment control, which is generally assigned according to previous research results combined with land use types (Zhou et al., 2019). However, compared with other soil and water conservation activities, check dams played a dominant role in sediment retention (Ran et al., 2008). To quantitatively analyze the influence of the check dam on sediment load, the trapping efficiencies of the dams were applied to evaluate the P factors. The detailed calculation process was based on the method proposed by Zhao et al. (2017).

According to Ferro and Porto (2000), the SDR value of each grid cell is calculated as follows:

$$\mathrm{SDR}_i = exp\left(-\beta \bullet t_i\right) = exp\left(-\beta \bullet \frac{l_i}{k_i\sqrt{s_i}}\right) (2)$$

where β is a coefficient that is affected by the roughness distribution along the flow path and is related to time.t_i is the travel time from cell i to the nearest stream reach, and l_i is the flow length (m). k_i is a coefficient dependent on surface roughness characteristics (m/s), and $s_i$represents the slope of the cell. The determination of the βvalue followed the method of Fu et al. (2006). To ensure the proper use of formula (2), the minimum value of s_i was set as 0.003 (Fernandez et al., 2003; Fu et al., 2006). The value ofk_i was extracted from previous studies (Fernandez et al., 2003; Gashaw et al., 2019).

To calibrate the model, in 2018, we selected two small check dams without a sluicing gate in the Kuye River watershed, and the sediment produced by soil erosion in the dam-controlled watershed was completely intercepted by the dams (*Fig. 3* a). Trench excavation was carried out on the dam land and the depth of sediment profile of the two dams reached 4.15m and 4.05m respectively. The flood couplets were then identified, divided and its thickness were measured (*Fig. 3* b). Finally, the capacity curve of check dams was reconstructed by the DEM of small watershed, and annual erosion modulus of the two dam-controlled watersheds from 2007 to 2018 were obtained by combining the soil bulk density of each flood couplets. The area-weighted average of the annual erosion modulus of the two dam-controlled watersheds was used as the annual erosion modulus for the whole Kuye River watershed from 2007 to 2018. For details of these two check dams, please refer to Zhang et al. (2020) and Wang (2020). However, it was very difficult to calibrate a model of such a large-scale watershed because the land use and the number of check dams changed continuously during the study period. To obtain a more realistic calculation, the sediment load was calculated for 1987 without considering the effect of check dams because the number of check dams and the total storage capacity were very limited (*Fig. 5*). The calculation of the annual erosion modulus and sediment load from 2006

to 2010 was based on the land use scenario in 2006 and included the effects of the check dams. The same method was applied from 2011-2016, except that the land use scenario was based on 2016. The annual erosion modulus measured from 2007-2016 was used to calibrate the RUSLE model. Additionally, the SEDD model simulation results were validated by using the observed sediment load of Wenjiachuan station in 1987 and from 2006-2016.

2.4 Distinguish the influence of different factors on soil erosion and sediment load

At the watershed scale of the Loess Plateau, soil erosion and sediment yield are mainly affected by climate variation and human activities. Human activities can be divided into land use changes affected by human activities and related soil and water conservation measures. Climate variation is mainly reflected in the change of precipitation, and check dams play a major role in sediment control in the study area (mentioned in the introduction of P factor). Therefore, we assumed that only three main driving factors (precipitation variation, land use changes and check dam construction) affect the soil erosion and sediment yield of the watershed. Taking the soil erosion and sediment load in 1987 as the reference year, the changes of soil erosion and sediment load during 1987-2006 and 1987-2016 were analyzed respectively. The calculation formula was as follows:

$$_T = (\mathrm{TSE}_i - \mathrm{TSE}_{1987}) \text{ or } (\mathrm{TSL}_i - \mathrm{TSL}_{1987}) =_P +_{\mathrm{LU}}+_{\mathrm{CD}} (3)$$

where *[?]*$_T$ is the total change of soil erosion or sediment load. TSE_i and TSL_i represent the total soil erosion and sediment load in ith year, respectively. TSE_{1987} and TSL_{1987}represent the total soil erosion and sediment load in 1987, respectively. *[?]*$_P$, *[?]*$_{LU}$ and*[?]*$_{CD}$ stand for the effects of precipitation variation (P), land use changes (LU) and check dams (CD), respectively.

The effects of precipitation variation and land use changes on soil erosion and sediment load can be distinguished by choosing different scenarios. The detailed calculation formula was shown in *Table 1* . Finally, the influence of check dams can be obtained by subtracting the influences of the other two factors from the total effects.

3. RESULTS

3.1 Land use changes

Fig. 4 shows that there were dramatic changes in land use, with the main conversion of arable land and bare land to grassland, shrubland, forestland and construction land. The proportion of vegetation coverage increased from 60% in 1987 to 86% in 2016. In addition, the urban and mining areas expanded rapidly from 9.62 km^2 in 1987 to 437.23 km^2 in 2016 (*Table 2*). This was mainly reflected in the urban expansion of Shenmu County, Dongsheng district and Yijinhuoqi County, as well as in the development of coal mines, which showed that the population, economy and urbanization had grown rapidly in the past three decades. In contrast, after decades of implementation and promotion of the abandonment of grazing and 'Grain for Green' policies, the area of arable land and bare land in the study presented a gradually decreasing trend. The area of arable land decreased from 2182.62 km^2 in 1987 to 533.71 km^2 in 2016. The proportion of bare land decreased from 13.43% in 1987 to 0.75% in 2016, and the area decreased by 1097.24 km^2.

3.2 Check dam construction

Fig. 5 shows the variation of the number and storage capacity of check dams on a time scale. The number and storage capacity of check dams showed similar change trend with time, both increased first and then decreased. In 2005, the annual number of dams and storage capacity reached the maximum, which were 42 and 41.61Mm^3 respectively. The accumulated number and storage capacity of check dams increased slowly before 2000, and then increased sharply. The turning point was mainly due to the 'Hydraulic highlight project' launched by the Ministry of Water Resources of China, which further increased the construction speed of check dams. Before 1987, only 32 check dams had been built, with a total storage capacity of 35.20 Mm^3. This shows that the interception capacity of check dams in 1987 was relatively limited. There were 306 key dams in the Kuye River watershed, with a total storage capacity of 316.64 Mm^3 until 2011.

3.3 Model calibration and validation

Fig. 6 a shows the model calibration using the annual erosion modulus, which was obtained through field excavation in 2018. The annual erosion modulus ranged from 39.88 to 64.02 t/ha/a, with an average value of 50.83 t/ha/a. Correspondingly, the simulated soil erosion modulus changed from 40.99 to 58.70 t/ha/a, with an average value of 49.48 t/ha/a. The R^2 reached 0.83, which indicated that the results of the model were, overall, in good agreement with the actual measured values.

Fig. 6 b shows the relationship between the measured and simulated annual sediment loads at Wenjiachuan station. The annual sediment loads in 1987 and from 2006-2016 were mainly simulated for model validation. The measured sediment load at Wenjiachuan station varied from 0.05 Mt in 2016 to 33.97 Mt in 1987, while the simulated annual average sediment load ranged from 8.55 Mt to 32.77 Mt. According to the fitting results of the scatter diagram ($R^2 > 0.90$), the simulation results of the model were basically consistent with the measured values, but compared with the measured values in recent years, the model tended to overestimate the sediment load.

3.4 Characteristics of soil erosion and sediment yield

Table 3 shows the classification of soil erosion and sediment yield under three different land use scenarios. According to the Chinese Soil Erosion Classification and Grading Standards (SL190–2007), the soil erosion grade changed from micro erosion to severe erosion. In 1987, the areas of micro, mild, moderate, intensive, extreme, and severe erosion accounted for 29.61%, 11.56%, 12.83%, 9.64%, 12.45% and 23.91%, respectively, of the area affected by erosion. The proportion of micro, mild, moderate, intensive, extreme, and severe erosion in 2016 was 59.68%, 11.38%, 8.80%, 5.44%, 6.08% and 8.61%, respectively. The area affected by mild or less serious erosion accounted for more than 70% of the whole watershed, which indicated that the soil erosion in the watershed had been well controlled by 2016. In 1987, the area of high erosion rates (>intensive) was 3981.29 km^2, accounting for 46% of the whole watershed area. In 2016, the area of high erosion rates was 1739.63 km^2, accounting for 20.14% of the whole watershed area. Nevertheless, compared with in 1987, the area with high erosion rates decreased by 2241.66 km^2 in 2016, and the area with severe erosion shrank by 1325.42 km^2. The results showed that the three factors played a remarkable role in reducing erosion.

The sediment yield was artificially divided into three grades: low, moderate and high sediment yield (*Table 3*). The distribution area of sediment yield under the three land use scenarios was low > moderate > high. Moreover, over time, the area occupied by the low sediment yield rate increased (from 4957.94 to 7276.03 km^2), while the others decreased. This indicated that sediment control in 2016 greatly improved under the influence of precipitation variation, land use changes and check dams.

The average SDR values in 1987, 2006 and 2016 were 0.32, 0.28 and 0.23, respectively, across the whole watershed, showing a decreasing trend. The results expounded that with the implementation of the 'Grain for Green' policy, land use changes had reduced the SDR.

Considering the check dams, we applied hot spot analysis (Getis-Ord Gi*) in ArcGIS software to analyze the soil erosion and sediment yield of the Kuye River watershed in 1987 and 2016 (*Fig. 7*). The distribution of cold and hot spots of soil erosion in 1987 and 2016 was consistent with that of sediment yield, and we found that the hot spots of soil erosion and sediment yield were mainly clustered around Shenmu County (*Fig. 1*). This indicated that the high-risk regions of soil erosion and sediment yield were mainly concentrated in the middle reaches of the watershed. However, the hot spot region in 2016 decreased compared with that in 1987. On the other hand, most of the cold spots were identified in Yijinhuoqi County, especially the sediment yield cold and hot spot maps of 2016 were the most obvious. This signified that the erosion degree in this area was relatively low.

3.5 The influence of different factors on soil erosion and sediment yield

Table 4 represents the contribution of three factors (precipitation variation, land use changes and check dams) to soil erosion and sediment yield in different periods. Compared with 1987, the total soil erosion in 2006 decreased by 57.74 Mt, and the contribution rates of the three factors were 8.61%, 20.44% and 70.95%,

respectively. In 2016, the total soil erosion decreased by 60.42 Mt, and the contribution rates of the three factors were 34.22%, 8.01% and 57.77%, respectively. This signified that check dams were the dominant factor, but its contribution rate to different years was diverse. In the past three decades, the impact of precipitation variation on the reduction of soil erosion had increased (from 8.61% in 2006 to 34.22% in 2016), while the impact of land use changes and check dams on soil erosion had decreased.

When compared with 1987, the total sediment load in 2006 and 2016 decreased by 21.50 Mt and 24.22 Mt, respectively, and the sediment load reduction in 2016 was greater. From 1987 to 2006, precipitation variation, land use changes and check dams reduced sediment load by 11.91%, 34.32% and 53.77% respectively. From 1987 to 2016, the contribution of these three factors to sediment reduction was 29.10%, 40.09% and 30.81%, respectively. The check dams were still the dominant factor in 2006, but the three factors all had obvious influence on sediment load in 2016. The influence of precipitation variation and land use changes on sediment load was increasing, while the influence of check dams on sediment load was decreasing.

4. DISCUSSION

4.1 Reasons for the change of contribution of three factors to soil erosion and sediment load reduction

By using the model to simulate different scenarios, we quantitatively distinguish the impact of three different factors on soil erosion and sediment load in different periods. In order to further explore the reasons for the change of contribution rate of precipitation variation to soil erosion and sediment load reduction, we separately analyzed the influence of precipitation variation on soil erosion and sediment yield (*Fig. 8*). The abscissa from low to high corresponds to the average R in 2016, 2006 and 1987 (903.58, 1117.52 and 1140.64 MJ·mm/ha·h). With the increase of precipitation, soil erosion modulus and sediment yield increased. Due to the largest reduction in precipitation in 2016, the impact of precipitation variation on soil erosion and sediment load also reached the maximum (*Table 4*). According to the slope of the graph, the impact of precipitation variation on erosion modulus is greater than that on sediment yield (*Fig. 8*). Therefore, compared with the impact on total sediment load reduction, precipitation variation has a greater impact on total soil erosion reduction (*Table 4*). In this study, the contribution of precipitation variation to sediment load reduction mainly changed from 11.91% to 29.09%, which was similar to the previous studies (Mu et al., 2012; Yang et al., 2018).

To further ascertain the primary factors leading to soil erosion and sediment yield reduction, we analyzed the contributions of different land use types to soil erosion and sediment yield (*Fig. 9*). In order to eliminate the impact of precipitation variation, we simulated all scenarios using the 1987 rainfall conditions. Without considering the effects of check dams, the amount of soil erosion in 1987 was mainly contributed by grassland, arable land and bare land, accounting for 40.90%, 26.09% and 13.04% of the total erosion, respectively. As of 2016, due to the increasing grassland area (*Table 2*), the amount of soil erosion caused by grassland increased slightly, and this land use type became the main source of soil erosion. In addition, as the area of arable land and bare land decreased rapidly, the contributions of these two land use types to soil erosion were significantly reduced by 21.72 Mt and 12.82 Mt, respectively. Therefore, without considering the roles of check dams, the reduction in soil erosion was mainly due to the change in the land use pattern, especially the conversion from arable land and bare land to vegetation land. Considering the action of check dams, the erosion amounts from grassland, arable land and bare land decreased by 52.77%, 57.12% and 42.92%, respectively, without land use changes in 1987. Under the three land use scenarios, the construction of check dams reduced the erosion of all land use types to varying degrees, and grassland had the largest erosion reduction.

In terms of sediment load, without considering the effect of check dams, the main sources of sediment in 1987 were arable land and bare land, accounting for 67.17% of the total sediment load. Nevertheless, grassland was no longer a major sediment source, indicating low sediment connectivity in the area. This development further led to less sediment that could be transported to the watershed outlet. Compared with 1987, the sediment contribution of arable land and bare land decreased significantly in 2016, with a reduction of more than 80%. Although the sediment loads of all land use types decreased to different degrees under the condition

of check dams, the conversion of land use played a more important role in the reduction in sediment load over time. This was due to the decrease of SDR caused by land use changes (mentioned above), so that the contribution of land use changes to sediment load reduction increased slightly over time (*Table 4*).

4.2 Impact of land use changes and check dams on sediment load

Many studies have applied various models and methods to clarify the impact of land use changes or check dams on sediment load in different regions of the world (*Table 5*). The land use of the Kuye River watershed has undergone dramatic changes in the past few decades, especially since the implementation of the Grain for Green Project in 1999. Nevertheless, land use change will significantly affects soil erosion and sediment transport (Fang, 2017). In this study, the conversion of arable land and bare land into vegetation land reduced the erosion of the source area and further decreased the sediment export by diminishing the SDR of the whole watershed. This was consistent with the results of Zhou et al., (2019). In contrast, when natural vegetation is artificially transformed into other land use types, such as cultivated land and urban land, the opposite result is obtained (Aneseyee et al., 2020; Sushanth and Bhardwaj, 2019).

As the main channel construction and important soil and water conservation engineering measures, check dams play a significant role in channeling watersheds, which can conserve water and soil, provide fertile farmland and prevent the downstream channel from scouring, reducing the downstream sediment load. Previous studies (Borja et al., 2018; Polyakov et al., 2014) have confirmed that check dams can maintain a significant proportion of the sediment load. Based on data from previous studies, Ran et al. (2008) indicated that in the Kuye River watershed, the reductions in sediment mass caused by check dams were 37.2% from 1970 to 1996. According to the results of this study, check dams reduced sediment export by 53.77% in 2006 and 30.81% in 2016. With the continued restoration of vegetation in the watershed, the contribution rate of check dam construction to sediment control may decrease slightly.

The SEDD model in this study overestimated the sediment load in recent years, which may be partly because only the key dams were considered but the small dams, terraces, concrete roads and other soil and water conservation measures were not considered. According to the results of the hot spot analysis, there were still some high-risk regions of soil erosion and sediment yield in this watershed, which may be mainly due to the rapid expansion of Shenmu County and the large-scale mining of coal resources in the surrounding area in recent decades. Then, these hot spot areas should become the focus for implementation of effective soil and water conservation measures to intervene with soil erosion. In addition, the vegetation coverage in this study area reached more than 80% in 2016 (*Table 2*), further reforestation will be difficult with the limitation of soil moisture. This implies that the impact of dams on sediment reduction will be very important in the future. On the other hand, the service life of the check dams was limited. Under extreme rainstorm conditions, check dams are prone to collapse and damage (Bai et al., 2020), releasing more sediment and producing serious disasters. In view of the existing circumstances, the operation status of check dams in the Kuye River watershed should be considered, and effective measures (such as spillway construction and dam reinforcement) for protecting check dams must be taken to guarantee the maximum efficiency of sediment interception.

5. CONCLUSIONS

This study analyzed the impacts of three factors on soil erosion and sediment yield in the Kuye River watershed by applying the SEDD model. The process of land use changes showed that arable land and bare land transformed into vegetation cover and construction land from 1987 to 2016, while arable land and bare land were the main sources of sediment yield in 1987. As of 2011, 306 key dams had been built in the Kuye River watershed, with a total storage capacity of 316.64 Mm^3. According to the classification of soil erosion and sediment yield, we found that under the influence of three factors, high erosion areas were consistently transformed into low erosion areas. Hot spot analysis showed that the high-risk regions of soil erosion and sediment yield were mainly concentrated in the middle reaches of the watershed, and the hot spots decreased with time. The average value of SDR for the whole watershed showed a declining trend with increasing time. The simulation results showed that the check dams were the dominant factor, reducing total soil erosion

by 70.95% in 2006 and 57.78% in 2016. Check dams reduced total sediment load by 53.77% in 2006, which were still the dominant factor. From 1987 to 2016, the contribution of these three factors to sediment load reduction was 29.10%, 40.09% and 30.81%, respectively, which indicated that all of them had significant influence on sediment load in 2016.

ACKNOWLEDGMENT

This study was financially supported by the Chinese Academy of Sciences "Light of West China" Program.

CONFLICT OF INTEREST

The authors declare no potential conflict of interest.

REFERENCES

Abedini, M., Md Said, M.A., Ahmad, F., 2012. Effectiveness of check dam to control soil erosion in a tropical catchment (The Ulu Kinta Basin). Catena 97, 63–70. https://doi.org/10.1016/j.catena.2012.05.003

Aneseyee, A.B., Elias, E., Soromessa, T., Feyisa, G.L., 2020. Land use/land cover change effect on soil erosion and sediment delivery in the Winike watershed, Omo Gibe Basin, Ethiopia. Sci. Total Environ. 728, 138776. https://doi.org/10.1016/j.scitotenv.2020.138776

Bai, L., Wang, N., Jiao, J., Chen, Yixian, Tang, B., Wang, H., Chen, Yulan, Yan, X., Wang, Z., 2020. Soil erosion and sediment interception by check dams in a watershed for an extreme rainstorm on the Loess Plateau, China. Int. J. Sediment Res. 35(4), 408–416. https://doi.org/10.1016/j.ijsrc.2020.03.005

Bellin, N., Vanacker, V., van Wesemael, B., Solé-Benet, A., Bakker, M.M., 2011. Natural and anthropogenic controls on soil erosion in the internal betic Cordillera (southeast Spain). Catena 87(2), 190–200. https://doi.org/10.1016/j.catena.2011.05.022

Boix-Fayos, C., de Vente, J., Martínez-Mena, M., Barberá, G.G., Castillo, V., 2008. The impact of land use change and check-dams on catchment sediment yield. Hydrol. Process. 22(25), 4922–4935. https://doi.org/10.1002/hyp.7115

Borja, P., Molina, A., Govers, G., Vanacker, V., 2018. Check dams and afforestation reducing sediment mobilization in active gully systems in the Andean mountains. Catena 165, 42–53. https://doi.org/10.1016/j.catena.2018.01.013

Bruijnzeel, L.A., 2004. Hydrological functions of tropical forests: Not seeing the soil for the trees?, Agriculture, Ecosystems and Environment. https://doi.org/10.1016/j.agee.2004.01.015

Cai, C., Ding, S., Shi, Z., Huang, L., Zhang, G., 2000. Study of Applying USLE and Geographical Information System IDRISI to Predict Soil Erosion in Small Watershed. J. Soil Water Conserv. 14(02), 20-24 (in Chinese). https://doi.org/10.13870/j.cnki.stbcxb.2000.02.005

Cai, J., Zhou, Z., Liu, J., Wang, H., Jia, Y., Xu, C.Y., 2019. A three-process-based distributed soil erosion model at catchment scale on the Loess Plateau of China. J. Hydrol. 578, 124005. https://doi.org/10.1016/j.jhydrol.2019.124005

Castillo, V.M., Mosch, W.M., García, C.C., Barberá, G.G., Cano, J.A.N., López-Bermúdez, F., 2007. Effectiveness and geomorphological impacts of check dams for soil erosion control in a semiarid Mediterranean catchment: El Cárcavo (Murcia, Spain). Catena 70(3), 416–427. https://doi.org/10.1016/j.catena.2006.11.009

Chen, L., Wei, W., Fu, B., Lü, Y., 2007. Soil and water conservation on the Loess Plateau in China: Review and perspective. Prog. Phys. Geogr. 31(4), 389–403. https://doi.org/10.1177/0309133307081290

Choukri, F., Raclot, D., Naimi, M., Chikhaoui, M., Nunes, J.P., Huard, F., Hérivaux, C., Sabir, M., Pépin, Y., 2020. Distinct and combined impacts of climate and land use scenarios on water availability and sediment loads for a water supply reservoir in northern Morocco. Int. Soil Water Conserv. Res. 8, 141–153. https://doi.org/10.1016/j.iswcr.2020.03.003

Fang, H., 2017. Impact of land use change and dam construction on soil erosion and sediment yield in the black soil region, Northeastern China. L. Degrad. Dev. 28(4), 1482–1492. https://doi.org/10.1002/ldr.2677

Fernandez, C., Wu, J.Q., McCool, D.K., Stöckle, C.O., 2003. Estimating water erosion and sediment yield with GIS, RUSLE, and SEDD. J. Soil Water Conserv. 58(3), 128–136.

Ferro, V., Minacapilli, M., 1995. Sediment delivery processes at basin scale. Hydrol. Sci. J. 40, 703–717. https://doi.org/10.1080/02626669509491460

Ferro, V., Porto, P., 2000. Sediment delivery distributed (SEDD) model. J. Hydrol. Eng. 5(4), 411–422. https://doi.org/10.1061/(ASCE)1084-0699(2000)5:4(411)

Fortugno, D., Boix-Fayos, C., Bombino, G., Denisi, P., Quiñonero Rubio, J.M., Tamburino, V., Zema, D.A., 2017. Adjustments in channel morphology due to land-use changes and check dam installation in mountain torrents of Calabria (southern Italy). Earth Surf. Process. Landforms 42(14), 2469–2483. https://doi.org/10.1002/esp.4197

Fu, B., Liu, Y., Lü, Y., He, C., Zeng, Y., Wu, B., 2011. Assessing the soil erosion control service of ecosystems change in the Loess Plateau of China. Ecol. Complex. 8(4), 284–293. https://doi.org/10.1016/j.ecocom.2011.07.003

Fu, G., Chen, S., McCool, D.K., 2006. Modeling the impacts of no-till practice on soil erosion and sediment yield with RUSLE, SEDD, and ArcView GIS. Soil Tillage Res. 85(1–2), 38–49. https://doi.org/10.1016/j.still.2004.11.009

Fu, S., Liu, B., Zhou, G., Sun, Z., Zhu, X., 2015. Calculation tool of topographic factors. Sci. Soil Water Conserv. 13(05), 109-114(in Chinese). https://doi.org/10.16843/j.sswc.2015.05.018

Gao, P., Deng, J., Chai, X., Mu, X., Zhao, G., Shao, H., Sun, W., 2017. Dynamic sediment discharge in the Hekou – Longmen region of Yellow River and soil and water conservation implications. Sci. Total Environ. 578, 56–66. https://doi.org/10.1016/j.scitotenv.2016.06.128

Gashaw, T., Tulu, T., Argaw, M., Worqlul, A.W., 2019. Modeling the impacts of land use–land cover changes on soil erosion and sediment yield in the Andassa watershed, upper Blue Nile basin, Ethiopia. Environ. Earth Sci. 78(24). https://doi.org/10.1007/s12665-019-8726-x

Jin, Z., Cui, B., Song, Y., Shi, W., Wang, K., Wang, Y., Liang, J., 2012. How many check dams do we need to build on the loess plateau? Environ. Sci. Technol. 46(12), 8527–8528. https://doi.org/10.1021/es302835r

Lantican, M.A., Guerra, L.C., Bhuiyan, S.I., 2003. Impacts of soil erosion in the upper Manupali watershed on irrigated lowlands in the Philippines. Paddy Water Environ. 1(1), 19–26. https://doi.org/10.1007/s10333-002-0004-x

Li, E., Mu, X., Zhao, G., Gao, P., Sun, W., 2017. Effects of check dams on runoff and sediment load in a semi-arid river basin of the Yellow River. Stoch. Environ. Res. Risk Assess. 31(7), 1791–1803. https://doi.org/10.1007/s00477-016-1333-4

Marques, M.J., Bienes, R., Pérez-Rodríguez, R., Jiménez, L., 2008. Soil degradation in Central Spain due to sheet water erosion by low-intensity rainfall events. Earth Surf. Process. Landforms 33(3), 414–423. https://doi.org/10.1002/esp.1564

Montgomery, D.R., 2007. Soil erosion and agricultural sustainability. Proc. Natl. Acad. Sci. U. S. A. 104, 13268–13272. https://doi.org/10.1073/pnas.0611508104

Mu, X., Zhang, X., Shao, H., Gao, P., Wang, F., Jiao, J., Zhu, J., 2012. Dynamic Changes of Sediment Discharge and the Influencing Factors in the Yellow River, China, for the Recent 90 Years. Clean - Soil, Air, Water 40(3), 303–309. https://doi.org/10.1002/clen.201000319

Polyakov, V.O., Nichols, M.H., McClaran, M.P., Nearing, M.A., 2014. Effect of check dams on runoff, sediment yield, and retention on small semiarid watersheds. J. Soil Water Conserv. 69(5), 414–421. https://doi.org/10.2489/jswc.69.5.414

Qiankun, G., Zhaowei, D., Wei, Q., Wenhong, C., Wen, L., Xiaomei, X., Zhe, Y., 2019. Changes in sediment load in a typical watershed in the tableland and gully region of the Loess Plateau, China. Catena 182, 104132. https://doi.org/10.1016/j.catena.2019.104132

Quiñonero-Rubio, J.M., Nadeu, E., Boix-Fayos, C., de Vente, J., 2016. Evaluation of the Effectiveness of Forest Restoration and Check-Dams to Reduce Catchment Sediment Yield. L. Degrad. Dev. 27(4), 1018–1031. https://doi.org/10.1002/ldr.2331

Ran, D.C., Luo, Q.H., Zhou, Z.H., Wang, G.Q., Zhang, X.H., 2008. Sediment retention by check dams in the Hekouzhen-Longmen Section of the Yellow River. Int. J. Sediment Res. 23(2), 159–166. https://doi.org/10.1016/S1001-6279(08)60015-3

Rao, E., Ouyang, Z., Yu, X., Xiao, Y., 2014. Spatial patterns and impacts of soil conservation service in China. Geomorphology 207, 64–70. https://doi.org/10.1016/j.geomorph.2013.10.027

Rey, F., Isselin-Nondedeu, F., Bédécarrats, A., 2005. Vegetation dynamics on sediment deposits upstream of bioengineering works in mountainous marly gullies in a Mediterranean climate (Southern Alps, France). Plant Soil 278(1–2), 149–158. https://doi.org/10.1007/s11104-005-8422-3

Romano, G., Abdelwahab, O.M.M., Gentile, F., 2018. Modeling land use changes and their impact on sediment load in a Mediterranean watershed. Catena 163, 342–353. https://doi.org/10.1016/j.catena.2017.12.039

Rustomji, P., Zhang, X.P., Hairsine, P.B., Zhang, L., Zhao, J., 2008. River sediment load and concentration responses to changes in hydrology and catchment management in the loess plateau region of china. Water Resour. Res. 45, 1–17. https://doi.org/10.1029/2007WR006656

Shi, P., Zhang, Y., Ren, Z., Yu, Y., Li, P., Gong, J., 2019. Land-use changes and check dams reducing runoff and sediment yield on the Loess Plateau of China. Sci. Total Environ. 664, 984–994. https://doi.org/10.1016/j.scitotenv.2019.01.430

Sun, P., Wu, Y., Wei, X., Sivakumar, B., Qiu, L., Mu, X., Chen, J., Gao, J., 2020. Quantifying the contributions of climate variation, land use change, and engineering measures for dramatic reduction in streamflow and sediment in a typical loess watershed, China. Ecol. Eng. 142, 105611. https://doi.org/10.1016/j.ecoleng.2019.105611

Sun, Q., Miao, C., Duan, Q., Wang, Y., 2015. Temperature and precipitation changes over the Loess Plateau between 1961 and 2011, based on high-density gauge observations. Glob. Planet. Change 132, 1–10. https://doi.org/10.1016/j.gloplacha.2015.05.011

Sushanth, K., Bhardwaj, A., 2019. Assessment of landuse change impact on runoff and sediment yield of Patiala-Ki-Rao watershed in Shivalik foot-hills of northwest India. Environ. Monit. Assess. 191(12). https://doi.org/10.1007/s10661-019-7932-z

Tang, Q., Xu, Y., Bennett, S.J., Li, Y., 2015. Assessment of soil erosion using RUSLE and GIS: a case study of the Yangou watershed in the Loess Plateau, China. Environ. Earth Sci. 73(4), 1715–1724. https://doi.org/10.1007/s12665-014-3523-z

Vanacker, V., von Blanckenburg, F., Govers, G., Molina, A., Poesen, J., Deckers, J., Kubik, P., 2007. Restoring dense vegetation can slow mountain erosion to near natural benchmark levels. Geology 35(4), 303–306. https://doi.org/10.1130/G23109A.1

Wang, G., 2020. Erosion Characteristics and Simulation in Typical Watersheds of More Sediment and Coarse Sediment Region in the Middle Reaches of the Yellow River (Dissertation, Hohai University).

Wang, Y., Fang, N., Tong, L., Shi, Z., 2017. Source identification and budget evaluation of eroded organic carbon in an intensive agricultural catchment. Agric. Ecosyst. Environ. 247, 290–297. https://doi.org/10.1016/j.agee.2017.07.011

Williams, J.R., Jones, C.A., Dyke, P.T., 1984. A modelling approach to determining the relationship between erosion and soil productivity. Trans. - Am. Soc. Agric. Eng. https://doi.org/10.13031/2013.32748

Wischmeier, W., Smith, D., 1978. Predicting rainfall erosion losses: a guide to conservation planning, U.S. Department of Agriculture Handbook No. 537. https://doi.org/10.1029/TR039i002p00285

Wu, X., Wang, H., Bi, N., Saito, Y., Xu, J., Zhang, Y., Lu, T., Cong, S., Yang, Z., 2020. Climate and human battle for dominance over the Yellow River's sediment discharge: From the Mid-Holocene to the Anthropocene. Mar. Geol. 425, 106188. https://doi.org/10.1016/j.margeo.2020.106188

Xin, Z., Ran, L., Lu, X.X., 2012. Soil Erosion Control and Sediment Load Reduction in the Loess Plateau: Policy Perspectives. Int. J. Water Resour. Dev. 28(2), 325–341. https://doi.org/10.1080/07900627.2012.668650

Xu, Y.D., Fu, B.J., He, C.S., 2013. Assessing the hydrological effect of the check dams in the Loess Plateau, China, by model simulations. Hydrol. Earth Syst. Sci. 17(16), 2185–2193. https://doi.org/10.5194/hess-17-2185-2013

Yang, X., Sun, W., Li, P., Mu, X., Gao, P., Zhao, G., 2018. Reduced sediment transport in the Chinese Loess Plateau due to climate change and human activities. Sci. Total Environ. 642, 591–600. https://doi.org/10.1016/j.scitotenv.2018.06.061

Yue, X., Mu, X., Zhao, G., Shao, H., Gao, P., 2014. Dynamic changes of sediment load in the middle reaches of the Yellow River basin , China and implications for eco-restoration. Ecol. Eng. 73, 64–72. https://doi.org/10.1016/j.ecoleng.2014.09.014

Zema, D.A., Bombino, G., Boix-Fayos, C., Tamburino, V., Zimbone, S.M., Fortugno, D., 2014. Evaluation and modeling of scouring and sedimentation around check dams in a Mediterranean torrent in Calabria, Italy. J. Soil Water Conserv. 69(4), 316–329. https://doi.org/10.2489/jswc.69.4.316

Zhang, W., Xie, Y., Liu, B., 2002. Rainfall erosivity estimation using daily rainfall amounts. Sci. Geogr. Sin. 22(6), 705-711 (In chinese).

Zhang, X., She, D., Wang, G., Huang, X., 2020. Source identification of soil elements and risk assessment of trace elements under different land uses on the Loess. Environ. Geochem. Health. https://doi.org/10.1007/s10653-020-00624-0

Zhao, G., Kondolf, G.M., Mu, X., Han, M., He, Z., Rubin, Z., Wang, F., Gao, P., Sun, W., 2017. Sediment yield reduction associated with land use changes and check dams in a catchment of the Loess Plateau, China. Catena 148, 126–137. https://doi.org/10.1016/j.catena.2016.05.010

Zhao, G., Mu, X., Jiao, J., An, Z., Klik, A., Wang, F., Jiao, F., Yue, X., Gao, P., Sun, W., 2016. Evidence and Causes of Spatiotemporal Changes in Runoff and Sediment Yield on the Chinese Loess Plateau. L. Degrad. Dev. 28(2), 579–590. https://doi.org/10.1002/ldr.2534

Zhao, Q., Wang, L., Liu, H., Zhang, Q., 2019. Runoff and sediment variation and attribution over 60 years in typical Loess Plateau basins. J. Soils Sediments 19(10), 3631–3647. https://doi.org/10.1007/s11368-019-02345-z

Zhou, M., Deng, J., Lin, Y., Belete, M., Wang, K., Comber, A., Huang, L., Gan, M., 2019. Identifying the effects of land use change on sediment export: Integrating sediment source and sediment delivery in the Qiantang River Basin, China. Sci. Total Environ. 686, 38–49. https://doi.org/10.1016/j.scitotenv.2019.05.336

Zuo, D., Xu, Z., Yao, W., Jin, S., Xiao, P., Ran, D., 2016. Assessing the effects of changes in land use and climate on runoff and sediment yields from a watershed in the Loess Plateau of China. Sci. Total Environ. 544, 238–250. https://doi.org/10.1016/j.scitotenv.2015.11.060

Table 1 Schemes for distinguishing the contribution of three factors to soil erosion and sediment load

Type	Period	$[?]_{\mathrm{P}}$	$[?]_{\mathrm{LU}}$	$[?]_{\mathrm{CD}}$
TSE	1987-2006	$T\mathrm{SE}_{R_{2006}C_{1987}} - \mathrm{TSE}_{R_{1987}C_{1987}}$	$\mathrm{TSE}_{R_{2006}C_{2006}} - \mathrm{TSE}_{R_{2006}C_{1987}}$	$T - P - \mathrm{LU}$
	1987-2016	$\mathrm{TSE}_{R_{2016}C_{1987}} - \mathrm{TSE}_{R_{1987}C_{1987}}$	$\mathrm{TSE}_{R_{2016}C_{2016}} - \mathrm{TSE}_{R_{2016}C_{1987}}$	$T - P - \mathrm{LU}$
TSL	1987-2006	$\mathrm{TSL}_{R_{2006}C_{1987}\mathrm{SDR}_{1987}} - \mathrm{TSL}_{R_{1987}C_{1987}\mathrm{SDR}_{1987}}$	$\mathrm{TSL}_{R_{2006}C_{2006}\mathrm{SDR}_{2006}} - T\mathrm{SL}_{R_{2006}C_{1987}\mathrm{SDR}_{1987}}$	$T - P - \mathrm{LU}$
	1987-2016	$T\mathrm{SL}_{R_{2016}C_{1987}\mathrm{SDR}_{1987}} - \mathrm{TSL}_{R_{1987}C_{1987}\mathrm{SDR}_{1987}}$	$\mathrm{TSL}_{R_{2016}C_{2016}\mathrm{SDR}_{2016}} - \mathrm{TSL}_{R_{2016}C_{1987}\mathrm{SDR}_{1987}}$	$T - P - \mathrm{LU}$

Notes: TSE and TSL represent total soil erosion and total sediment load respectively. $[?]_P$, $[?]_{LU}$ and$[?]_{CD}$ stand for the effects of precipitation variation (P),

land use changes (LU) and check dams (CD), respectively.

Table 2 Land use types and changes in the Kuye River watershed

Land use types	1987	1987	2006	2006	2016	2016	Changes (1987-2006)	Changes (1987-2006
	km^2	%	km^2	%	km^2	%	km^2	%
Water bodies	34.43	0.40	68.11	0.79	75.11	0.87	33.68	0.39
Grass land	2785.51	32.20	3341.47	38.62	3789.98	43.81	555.95	6.43
Forests	1114.21	12.88	1935.77	22.38	1981.14	22.90	821.57	9.50
Arable land	2182.62	25.23	1065.12	12.31	533.71	6.17	-1117.50	-12.92
Shrub land	1362.96	15.75	1524.27	17.62	1769.43	20.45	161.31	1.86
Urban and mining area	9.62	0.11	403.45	4.66	437.23	5.05	393.83	4.55
Bare land	1161.98	13.43	313.13	3.62	64.74	0.75	-848.85	-9.81

Table 3 Classification of soil erosion and sediment yield

Soil erosion grade	Soil erosion grade	Micro	Mild	Moderate	Intensi
1987	area/km^2	2562.21	1000.08	1110.72	833.94
	percentage/%	29.61%	11.56%	12.83%	9.64%
2006	area/km^2	4930.45	1002.94	829.68	509.81
	percentage/%	57.07%	11.61%	9.60%	5.90%
2016	area/km^2	5156.11	982.80	760.44	470.24
	percentage/%	59.68%	11.38%	8.80%	5.44%
Sediment yield grade	Sediment yield grade	Low (0-10 t/ha/a)	Low (0-10 t/ha/a)	Moderate (10-50 t/ha/a)	Moder
1987	area/km^2	4957.94	4957.94	2030.94	2030.9
	percentage/%	57.29%	57.29%	23.47%	23.47%
2006	area/km^2	7001.38	7001.38	1097.54	1097.5
	percentage/%	81.05%	81.05%	12.72%	12.72%
2016	area/km^2	7276.03	7276.03	962.65	962.65
	percentage/%	84.23%	84.23%	11.15%	11.15%

Chinese soil erosion classification and grading standards (SL190–2007): water erosion (a) micro (< 2, < 5, $<$ 10 t/ha/year), (b) mild (10–25 t/ha/year), (c) moderate (25–50 t/ha/year), (d) intensive (50–80 t/ha/year), (e) extremely intensive (80–150 t/ha/year), and (f) severe (>150 t/ha/year)

Table 4 Contribution of three factors to soil erosion and sediment yield

Type	Period	Precipitation variation	Precipitation variation	Land use changes	Land use changes	Check dams
		Reduction	Contribution(%)	Reduction	Contribution(%)	Reduction
TSE	1987-2006	-4.97	8.61	-11.80	20.44	-40.97
	1987-2016	-20.67	34.22	-4.84	8.01	-34.91
TSL	1987-2006	-2.56	11.91	-7.38	34.32	-11.56
	1987-2016	-7.05	29.10	-9.71	40.09	-7.46

Notes: The unit for total soil erosion (TSE) and total sediment load (TSL) reduction is Mt.

Table 5 Studies on the influence of check dams and land use changes on sediment yield

Reference	Watershed area (km^2)	Location	Method
Boix-Fayos et al., 2008	47.2	Rogativa catchment in Spain	WaTEM/S
Ran et al., 2008	8651	Kuye River basin in China	Data colle
	4161	Sanchuan River basin in China	Data colle
Xu et al., 2013	7725	Yanhe Watershed in China	SWAT mo
Polyakov et al., 2014	0.04/0.031	Santa Rita Experimental Range in the United States	Field samp
Zema et al., 2014	17.43	Fiumara Sant'Agata in Italy	Field samp
Zuo et al., 2016	3246	Huangfuchuan Watershed in China	SWAT mo
Quiñonero-Rubio et al., 2016	320	Upper Taibilla catchment in Spain	WaTEM/S
Fortugno et al., 2017	26.1	Fiumara Sant'Agata in Italy	Field surve
Zhao et al., 2017	3246	Huangfuchuan Watershed in China	SEDD mo
Li et al., 2017	3246	Huangfuchuan Watershed in China	SWAT mo
Fang, 2017	915	Shuangyang catchment in China	WaTEM/S
Borja et al., 2018	0.002-0.047	Loreto catchment in the Andean mountains	Field surve
Romano et al., 2018	506	Carapelle watershed in Italy	AnnAGNP
Shi et al., 2019	30261	Wuding River Watershed in China	SWAT mo
Guo et al., 2019	369	Yanwachuan watershed in China	SEDD mo
Zhou et al., 2019	42700	Qiantang River Basin in China	InVEST m
Sushanth and Bhardwaj, 2019	51.4	Patiala-Ki-Rao watershed in India	WEPP mo
Aneseyee et al., 2020	1091.8	Winike watershed in Ethiopia	InVEST m
Choukri et al., 2020	180	Tleta watershed in Morocco	SWAT mo
Sun et al., 2020	774	Zhou River Basin in China	SWAT mo

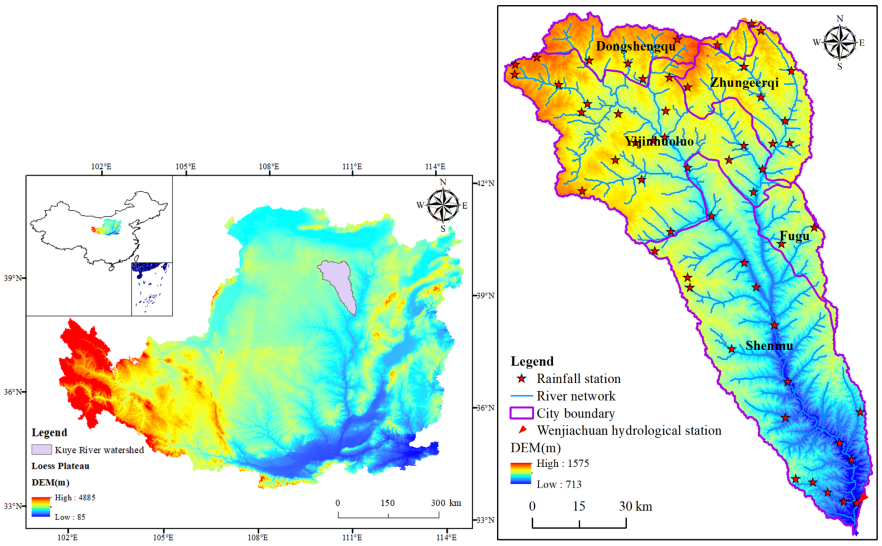

Fig. 1. Location of the Kuye River watershed.

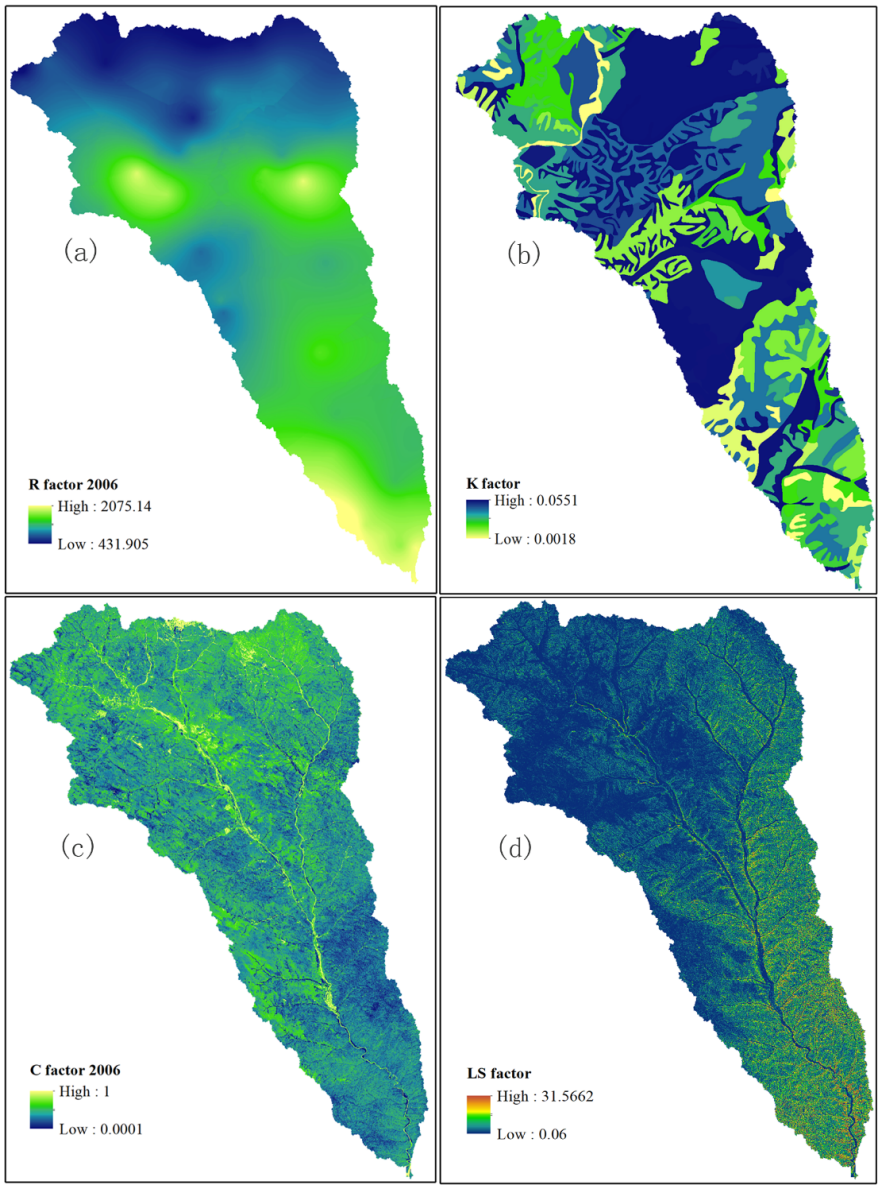

Fig. 2. Model factors of the Kuye River watershed.

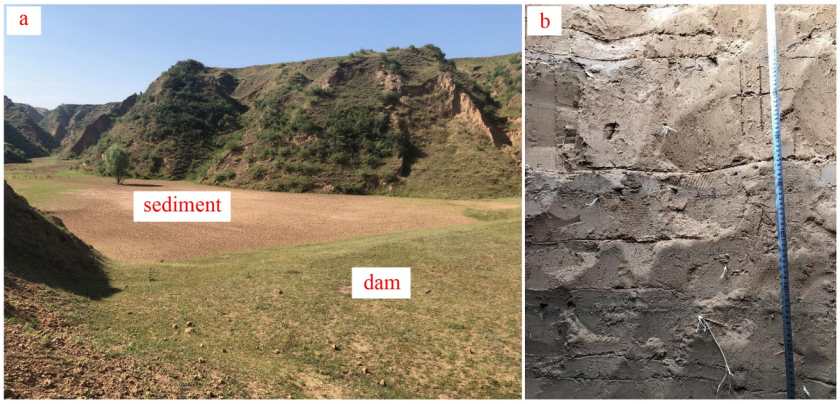

Fig. 3. Check dams selected in Kuye River watershed. a) check dams without a sluicing gate. b) sediment profile in the check dam.

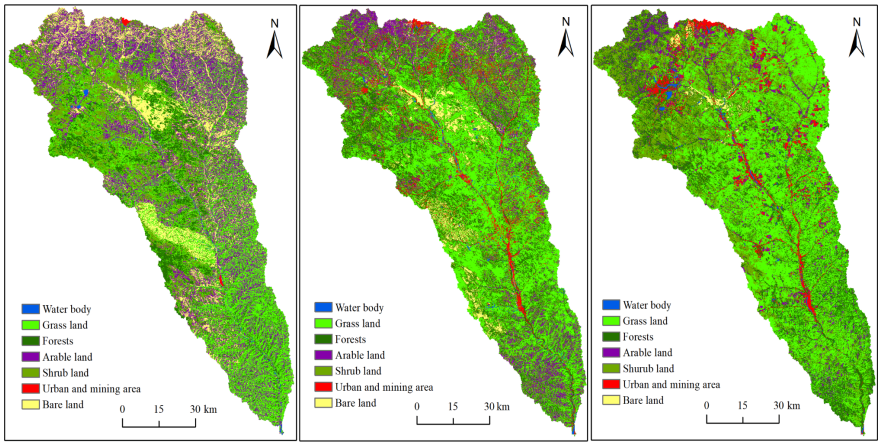

Fig. 4. Land use changes in the Kuye River watershed

Fig. 5. Status of the check dam construction in the Kuye River watershed, a) change of the number and accumulated number of dams with time, b)change of storage capacity and accumulated storage capacity with time

Fig. 6. Comparison of the measured and simulated values a) soil erosion estimation through check dam siltation and RUSLE modeling and b) sediment load simulation at the Wenjiachuan gauge.

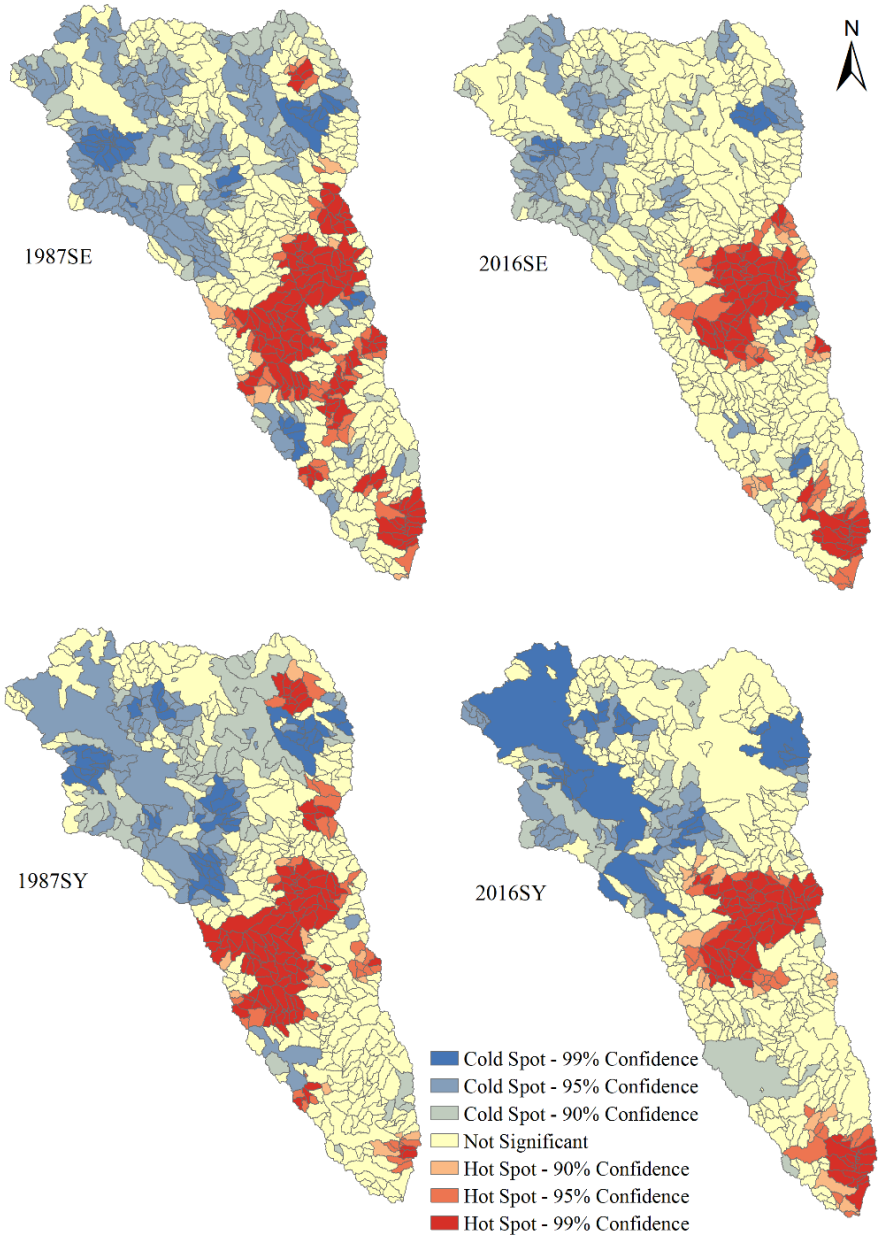

Fig. 7. Spatial distribution of hot spots and cold spots of soil erosion (SE) and sediment yield (SY) in 1987 and 2016.

Fig. 8. Influence of precipitation variation on average soil erosion and average sediment yield of the whole watershed

Fig. 9. Total values of soil erosion and sediment load for different land use types from 1987-2016